

See discussions, stats, and author profiles for this publication at: <https://www.researchgate.net/publication/315639966>

Cassava Leaf Nanoparticles (CLNPs) as a Potential Additive to Anti-Corrosion Coatings for Oil and Gas Pipeline

Article in Tribology in Industry · March 2017

DOI: 10.24874/ti.2017.39.01.07

CITATIONS

0

READS

116

7 authors, including:



Funsho Kolawole

Federal University Oye-Ekiti

12 PUBLICATIONS 9 CITATIONS

[SEE PROFILE](#)



Johnson Olumuyiwa Agunsoye

University of Lagos

63 PUBLICATIONS 228 CITATIONS

[SEE PROFILE](#)



Jeleel Adekunle ADEBISI

University of Ilorin

36 PUBLICATIONS 22 CITATIONS

[SEE PROFILE](#)



Bolaji Hassan

University of Lagos

42 PUBLICATIONS 449 CITATIONS

[SEE PROFILE](#)

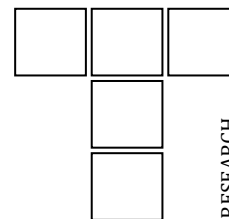
Some of the authors of this publication are also working on these related projects:



Mathematical Prediction and Size validation of Nanoparticles obtained from Coconut Shells using Regression Analysis [View project](#)



Utilization of Abattoir Wastes for Heat Treatment of Steels [View project](#)



Cassava Leaf Nanoparticles (CLNPs) as a Potential Additive to Anti-Corrosion Coatings for Oil and Gas Pipeline

F.O. Kolawole^{a,b}, S.K. Kolawole^{c,d}, J.O. Agunsoye^b, S.A. Bello^{b,e}, J.A. Adebisi^{b,f}, O.C. Okoye^g, S.B. Hassan^b

^aDepartment of Materials and Metallurgical Engineering, Federal University Oye-Ekiti, Nigeria,

^bDepartment of Metallurgical and Materials Engineering, University of Lagos, Lagos, Nigeria,

^cAfrican University of Science and Technology, Abuja, Nigeria,

^dNational Agency for Science and Engineering Infrastructure, Abuja, Nigeria,

^eDepartment of Materials Science and Engineering, Kwara State University, Malete, Nigeria,

^fDepartment of Metallurgical and Materials Engineering, University of Ilorin, Ilorin, Nigeria,

^gDepartment of Mechanical Engineering, Federal University Oye-Ekiti, Nigeria.

Keywords:

Cassava
Characterization
Leaf
Nanoparticles
Synthesis
Coatings

ABSTRACT

Characterization of synthesized cassava leaf nanoparticles (CLNPs) was carried out using SEM/EDX and Gwyddion software, XRD and TEM for cassava leaves (CL) ball milled at 36, 48, 60 and 72 hours. The morphological study was done using SEM and the Gwyddion software was used to determine the particle sizes from the SEM images. The particle size range for the un-milled cassava leaves (CL) was between 1.88 ± 0.09 to $19.53 \pm 0.98 \mu\text{m}$. After milling for 36, 48, 60 and 72 hours the average particle sizes were 4.96 ± 0.25 , $3.51 \pm 0.18 \mu\text{m}$, 86.90 ± 4.35 , $74.50 \pm 3.73 \text{ nm}$ respectively. Crystallite size of $23.94 \pm 1.20 \text{ nm}$ was obtained by XRD using Scherrer equation after milling for 72 hours and the XRD results revealed the presence of compounds such as SiO_2 , CaCO_3 , $\text{Ca}_2(\text{SO}_4)_2\text{H}_2\text{O}$ and $\text{CaC}_2\text{O}_4(\text{H}_2\text{O})$. Furthermore, TEM was used to determine nanoparticles after milling for 72 hours and the particle size ranged from 9.16 ± 0.46 to $58.20 \pm 2.91 \text{ nm}$ for cassava leaf nanoparticles (CLNPs) and EDX results showed trace element of O, Si, Ca, K, Fe and S in the CL milled for 72 hours. FTIR was also carried out to determine the nature of bond that exist in the organic compounds in CLNPs and GCMS analysis was used to reveal the organic compounds that were present in CLNPs. Anti-Corrosion coatings reduces corrosion activities to the bearest minimum.

Corresponding author:

F.O. Kolawole
Department of Materials and
Metallurgical Engineering, Federal
University, Oye-Ekiti, Nigeria
E-mail: funsho.kolawole@fuoye.edu.ng

© 2017 Published by Faculty of Engineering

1. INTRODUCTION

Cassava leaves (CL) are sometimes considered as agricultural waste (agro-waste), though they have other applications such as animal feed [1,2], medicinal application [1] and they are

used in pack-cyaniding of mild steel [2]. Cassava leaves are also known for their high hydrogen cyanide (HCN) content, low energy, bulkiness and their high tannin content [1,2]. Cassava leaves are nutritionally valuable products and cassava plant could yield 7-15 tonnes of leaves

per hectare, which accounts for an additional one tonne of valuable protein and 2.5 tonnes of carbohydrate per hectare [1]. Cassava leaves consist of up to 6 % of the entire cassava plant [1]. Cassava leaves are in abundance globally, since the world production of cassava is estimated to be 245 million tonnes annually with African producing about 138 million tonnes and of which Nigeria produces 54 million tonnes [3]. The world annual agro-waste generated is estimated to be about 140 billion metric tonnes [4], which is sufficient for bio-gas, animal feed, bio-fertilizer, pulp and paper, leather, alcohol production and engineering applications [5-9]. Agro-waste, if not put into proper use can cause problems. Where such waste litter the environment; usually block drainages and also providing conducive conditions for mosquitoes to breed. [5,10,11]. But if they are put into proper use they can create wealth for individuals, result in a cleaner environment, create jobs and better the standard of living [12].

The use of food items for corrosion inhibitors should be strongly discouraged as plants parts naturally synthesize chemical compounds in defence against fungi, insects and herbivorous mammals. Some of these compounds or phytochemicals such as alkaloids, terpenoids, flavonoids, polyphenols and glycosides prove beneficial to humans in unique manner for the treatment of several diseases. These compounds are identical in structure and function to conventional drugs. Extracts from parts of plants such as roots, stems, and leaves also contain such extraordinary phytochemicals that are used as pesticides, antimicrobials, drugs and herbal medicines [13-16], and can also be used as corrosion inhibitor in coatings because of the presence of heteroatoms and organic compounds.

Numerous coatings have been developed to prevent corrosion and enhance the service life of engineering components [17-21]. The effects of nanoscale can be used to create coatings with significantly optimized or enhanced corrosion properties. Nanostructured coating has the potentials for corrosion protection, and surface coating technology can be used to achieve corrosion-resistant. Nanostructured coatings play an important role in protecting the structural metals [22-25].

Nanoparticles which have a wide range of applications in bio-medical, composites, solar cells and engineering applications are being processed through two (2) major approaches, namely; top-down method and bottom-up method [26-29]. Since, most agro-wastes are used for engineering applications; agro-waste can be processed into nanoparticles for various applications [26,27] Bello et al. [30] reported the synthesis of uncarbonised coconut shell nanoparticles. Coating is one of the most efficient methods used for combating corrosion in the oil and gas industry [31-33]. Coatings may be applied alone or may be used with other common methods such as proper material selection, cathode protection (CP) and application of inhibitors to modify the corrosive environment [34,35]. Anti – corrosion coatings generally operate mainly be three mechanisms namely; barrier creation between substrate materials and environments, inhibition of the corrosion processes, and coating acting as sacrificial materials. However, recently one of the newest approaches is what is called “active-passive”. Here the coating acts as a barrier layers which will not allow permeation of corrosive agents to the metal surface (passive). While the active approach allows the formation of effective passive layer and this will impedes the corrosion half reactions leading to Schottky barrier at the interface resulting in depletion of electrons [21]. Nanoparticles can be incorporated as additives in coatings to inhibit corrosion. Incorporating nanosize additives in coatings provide effective barrier performance, reduce the amount of holiday in coatings and also enhance the integrity and durability of coatings. Since the fine particles dispersed in coatings can fill cavities and extract from cassava leaf contains organic compound in them, these will further improve metallic coating properties.

In this research cassava leaves nanoparticles (CLNPs) were synthesized from cassava leaves (CL) using top-down approach (ball milling). The CL were milled at different milling times (36, 48, 60 and 72) hours and characterized using scanning electron microscope (SEM) attached with EDX and Gwyddion software, X-ray diffraction spectroscopy (XRD) and transmission electron microscope (TEM).

2. Materials, Equipment and Methodology

2.1 Materials and Equipment

Cassava leaves (CL) which were used for this work were obtained from farmers in Ayedun-Ekiti, Nigeria. Equipment used includes grinding machine in Ilorin, Kwara State, Nigeria and ball milling machine in Federal Institute of Industrial Research Oshodi (FIIRO), Lagos, Nigeria. Sieve shaking machine and digital weighing scale in Federal University of Technology Akure (FUTA), Akure, Nigeria. Other equipment used were scanning electron microscope (SEM) attached with EDX and Gwyddion software, X-ray diffraction spectroscope (XRD) and transmission electron microscope (TEM) in University of Pretoria, South Africa.

2.2 Methodology

Synthesis of cassava leaf nanoparticles

Cassava leaves were soaked in water for 24 hours (see Fig. 1a), in order to reduce the level of cyanide content. After which the cassava leaves were sun dried for 14 days (see Fig. 1b). The dried cassava leaves were ground using a grinding machine. Thereafter they were sieved using a sieve shaking machine for 1 hour, the sieve size range from 150 to 53 μm .



Fig. 1. Image of cassava leaves (a) soaked in water (b) sun dried (c) powder milled for 72 hours.

200 g of CL powder was placed in an E3 sized vial containing 5 to 600 mm sized ceramic balls having a total mass of 2 kg. The CL powder was milled for 36, 48, 60 and 72 hours. Figure 1c shows cassava leaves milled for 72 hours. Each

day the cassava leaves were milled for 6 hours. The milling was carried out at a speed of 195 rpm, under dry grinding condition. Samples were taken from each of the powder at the different milling time intervals stated above for analysis.

Characterization of CLNPs

Scanning electron microscope (SEM) with EDX/Gwyddion software was used to study the particle size, morphology and chemical element of all the samples at the different time intervals. X-ray diffraction spectroscopy (XRD) was used to determine the compounds present and to analyze the particle size of the CLNPs. Transmission electron microscope (TEM) was used to have a more precise particle size analysis, by viewing the microstructure at a higher resolution.

SEM/EDX

The SEM was obtained using a Zeiss Ultra Plus 55 field emission scanning electron microscope (FE-SEM) operated at an accelerating voltage of 2.0 kV. EDX was performed with the same system operated at 20 kV. SEM images were taken for un-milled sample and for the milled samples which were milled for (36, 48, 60 and 72 hours) respectively. Gwyddion software was used to determine the minimum, maximum, average and median particle size of the SEM images for both un-milled and milled samples. Furthermore, EDX was used to determine trace elements in CL after 72 hours of milling.

XRD

Powder X-ray diffraction (XRD) was recorded in the 2θ range between 20.0–80.0 using an XPERT-PRO diffractometer (PANalytical BV, the Netherlands) with theta/2theta geometry and a counting time of 15.240 seconds per step. Qualitative phase analysis of samples was conducted with the X'pert Highscore search match software at room temperature using Co $k_{1\alpha}$ ($\lambda=0.178897$ nm). XRD was used to analyze samples of CL milled for 72 hours, the particle size was estimated using Scherrer equation (see equation 1) as reported by Monshi, et al, 2012 [31].

$$L = \frac{\kappa\lambda}{\beta\cos\theta} \quad (1)$$

where L is particle size, λ is the X-ray wavelength in nanometer (nm), β is the peak width of the diffraction peak profile at half maximum height resulting from small crystallite size in radians, and K is a constant related to crystallite shape, normally taken as 0.9. The value of β in 2θ axis of diffraction profile must be in radians [36]. The wavelength used for the samples was $\lambda\text{Cok}\alpha_1 = 0.178897$ nm.

TEM

TEM was carried out using JEOL Transmission Electron Microscope (Model: JEM-2100F Multipurpose Field Emission TEM) to analyze samples of cassava leaves milled for 72 hours, in order to determine the particle size.

FTIR

Fourier-Transform Infrared (FTIR) spectra were recorded on a Vertex 70v (Bruker) spectrometer in the $4000\text{--}500\text{ cm}^{-1}$ range with 4 cm^{-1} resolution and analyzed with the Opus software.

GC-MS

The dried CSNPs were soaked in ethanol for 72 hours to allow proper extraction. Soxhlet extraction processes using ethanol as extraction solvents were carried out; 350 mL of solvent was poured into the round bottom extraction flask, and placed on the heating mantle. After this, the thimble containing the sample was placed into the extraction chamber. Lastly, the condenser was placed on top of the extraction flask and all these parts were fixed vertically. The extraction was carried out for 6 hours. The extract was stored in a refrigerator at the temperature below $4\text{ }^{\circ}\text{C}$ until analyzed Gas Chromatography Mass Spectroscopy (GC-MS) after the soxhlet extraction process.

3. Results and Discussions

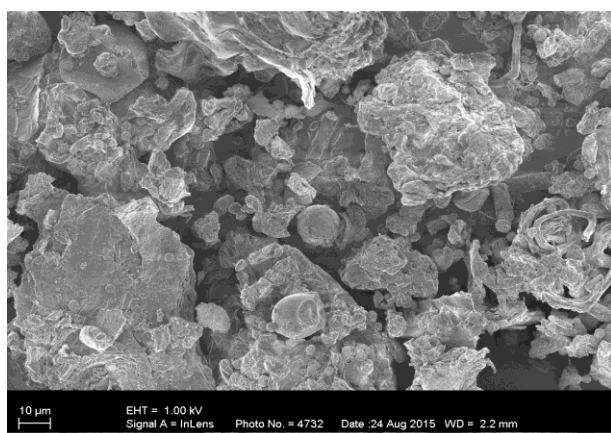
3.1 SEM micrographs

The morphology of the un-milled CL shown in Fig. 2a, reveals microstructures of CL having random particle size and shape. The presence of random particle sizes and shapes was due to the fact that grinding was carried out only for a short time.

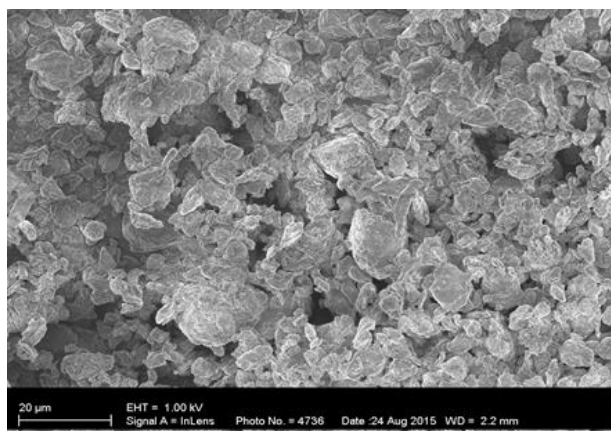
The morphology of CL milled for 36 hours shown in Fig. 2b, revealed microstructure of CL powder obtained at 36 hours of milling having random particle size and shape with few of them being spherical. The microstructure also reveals agglomeration of fine particles and discrete fine particles. At this stage of milling the CL powder particles were flattened by the compressive forces due to the collision of the ceramic balls. The appearance of agglomerated fine particles and discrete particles may be as a result of repeated impact of the ceramic balls on the CL powder particles with high kinetic energy. Figure 2c shows the SEM micrograph of cassava leaves milled for 48 hours. The microstructure in Fig. 2c reveals agglomeration of fine particles and discrete fine particles. After 48 hours of milling the cassava leaves powder particles, there was a reduction in random particle size and shape as some of the particles were spherical. There was also an increase in agglomeration of particles, this may be as a result of continuous fracturing and cold welding of the cassava leaves powder particles. The cold welding of the fine particles may be attributed to the heat generated during the impact of the ceramic balls on the cassava leaves and the wall of the vial which was high enough to produce moisture that led to cold welding. Figure 2d shows the SEM micrograph of cassava leaf nanoparticles (CLNPs) obtained at 60 hours of milling. The microstructure in Fig. 2d reveals a higher degree of agglomerated fine particles and few discrete fine particles. There was also an appearance of more uniform particle size and shape. The uniformity in particle size and shape may be as a result of continuous fracturing of fine particles by the impact of the ceramic balls. Although agglomeration occurred due to cold welding of fine particles, but continuous impact of the ceramic balls made it possible for fracturing of agglomerated particles. CLNPs were observed after milling for 60 hours. This may be attributed to an increase in milling time, which led to continuous fracturing and cold welding of the CL. Figure 2e shows the SEM micrograph of CLNPs obtained at 72 hours of milling. The microstructure in Fig. 2e reveals the highest degree of agglomeration of fine particles (nanoparticles) and fewer discrete fine particles. This may be attributed to an increase in impact time by the ceramic ball on the CLNPs, as a higher degree of heat was generated leading to more moisture in the vial container thereby

causing discrete fine particles to cold weld on already agglomerated particles causing bigger agglomerated particles and also resulting to fewer discrete fine particles. It can also be observed that the smallest particle size was obtained after milling for 72 hours compared to those milled at lesser hours.

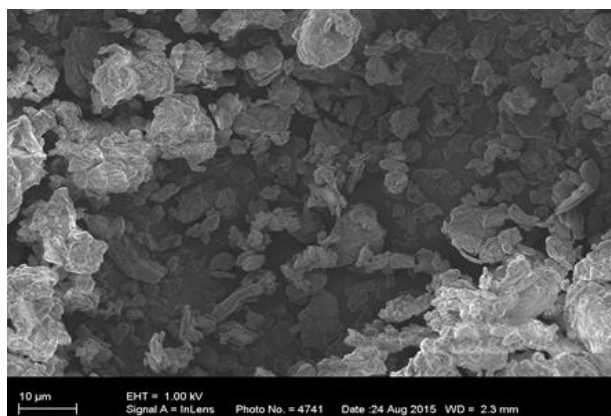
Figure 2f shows the EDS spectrograph of the CLNPs obtained at 72 hours of milling, the EDS spectrograph in Fig. 2f indicates the presence of O, Si, Ca, K, Fe and S (Table 1).



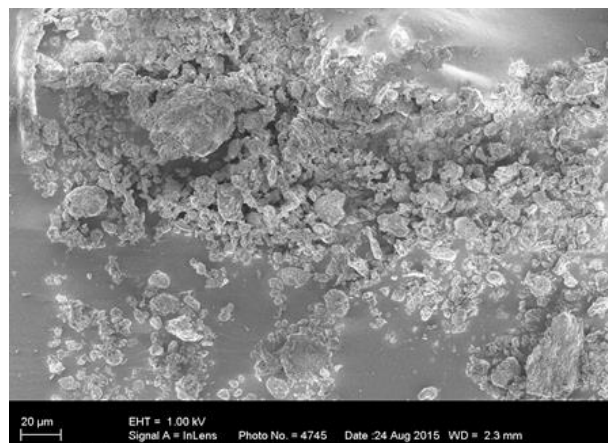
a)



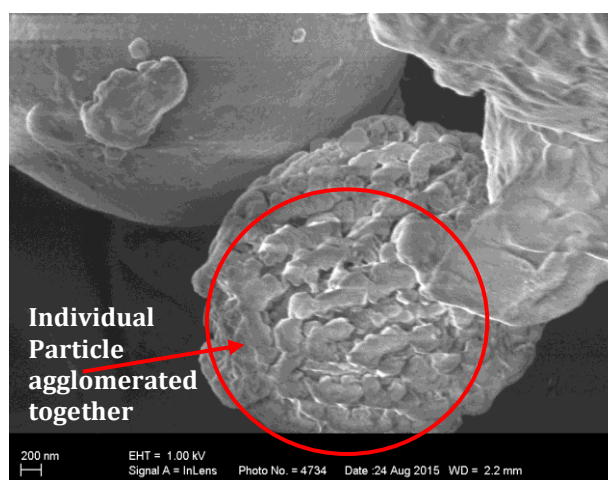
b)



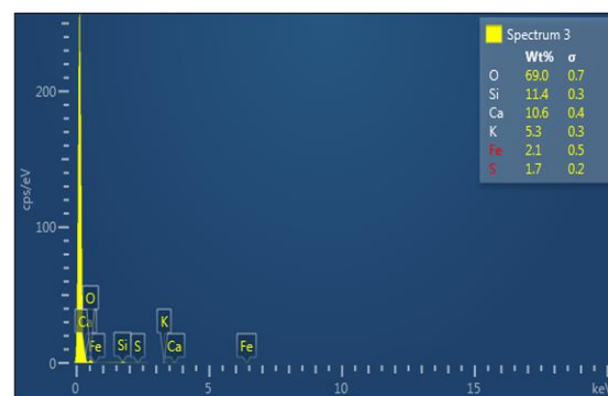
c)



d)



e)



f)

Fig. 2. SEM of cassava leaf (a) un-milled (b) milled for 36 hours (c) milled for 48 hours (d) milled for 60 hours (e) milled for 72 hours (f) EDX of CL milled for 72 hours.

Table 1. EDS Chemical Analysis of CLNPs milled for 72 hours.

Elements	% Composition
O	69.0
Si	11.4
Ca	10.6
K	5.3
Fe	2.1
S	1.7

Heteroatoms which are present in the cassava leave powder when added to coatings can help in inhibiting corrosion on metal surfaces. Elements like Si and Ca would improve the strength coatings as well as reduce the corrosion rate as reported by Shi et al, 2009 [31].

Figure 3, shows the particle size distribution and the particle size obtained was analyzed using SEM supported with Gwyddion software. The minimum, maximum, average and median particle sizes for the un-milled CL were 1.88 ± 0.09 , 19.53 ± 0.98 , 10.53 ± 0.53 and 10.67 ± 0.53 μm respectively. The average particle size obtained were 4.96 ± 0.25 μm , 3.51 ± 0.18 μm , 86.90 ± 4.35 nm and 74.50 ± 3.73 nm for CL milled for 36, 48, 60 and 72 hours, respectively. The results also revealed nanoparticles were obtained after milling for 60 hours. From the bar chart, it can be seen that as milling time increases, there was a decrease in particle size, the minimum particle size that was obtained for the un-milled sample, and for samples milled for 36, 48, 60 and 72 hours respectively were 1.88 ± 0.09 , 0.94 ± 0.05 , 0.86 ± 0.04 μm , 30.60 ± 1.53 nm and 27.50 ± 1.38 nm respectively (Fig. 3).

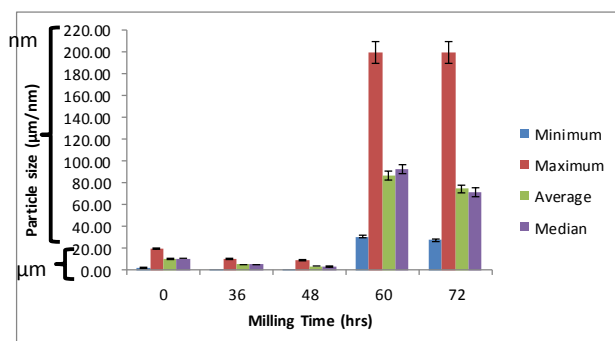


Fig. 3. Bar chart showing the minimum, maximum, average and median particle size of CLNPs

3.2 XRD analysis

From the XRD result shown in Fig. 4, the major peaks occurred at diffraction angles (2θ) of 24.3° , 30.7° , 31° and 34.5° , corresponding to $\text{CaC}_2\text{O}_4(\text{H}_2\text{O})$, $\text{Ca}_2(\text{SO}_4)_2\text{H}_2\text{O}$, SiO_2 and CaCO_3 respectively. Peaks representing each phase are indicated by vertical lines in different colours for the purpose of phase identification. The most intensified peak which occurred at 31° was used to estimate the particle size using Scherrer equation (see equation 1). The particle size of CL obtained after milling for 72 hours was 23.94 ± 1.20 nm. The XRD results using the Scherrer

equation indicates that CLNPs were obtained at 72 hours of milling. The presence of SiO_2 in coatings will improve the coatings hardness, while the presence of CaCO_3 in coatings will form a precipitate that will serve as a protective film on the surface of metal, thereby protecting the metal from corrosion.

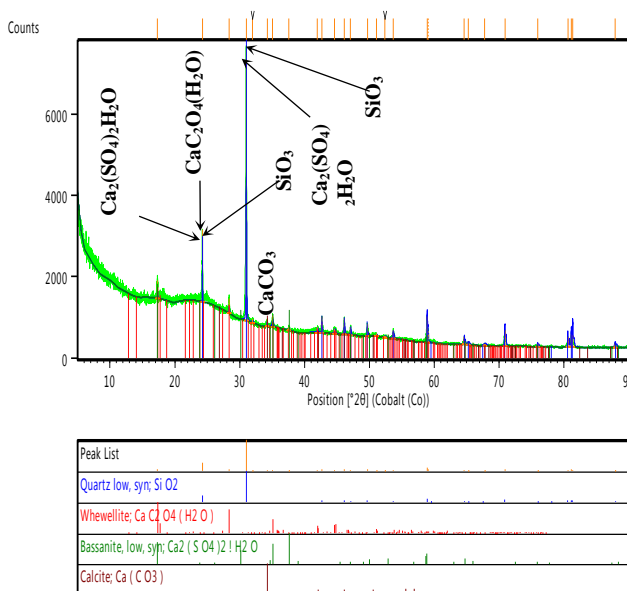


Fig. 4. XRD of CLNPs obtained after milling for 72 hours.

3.3 TEM micrographs

The TEM image which was taken for CL milled at 72 hours at a resolution of 100 nm shown in Fig. 5, revealed a more precise particle size compared to that obtained from SEM. The particles were spherical in shape. This was determined by placing a red perpendicular line at the centre of the particle from top to bottom as shown in the TEM images.

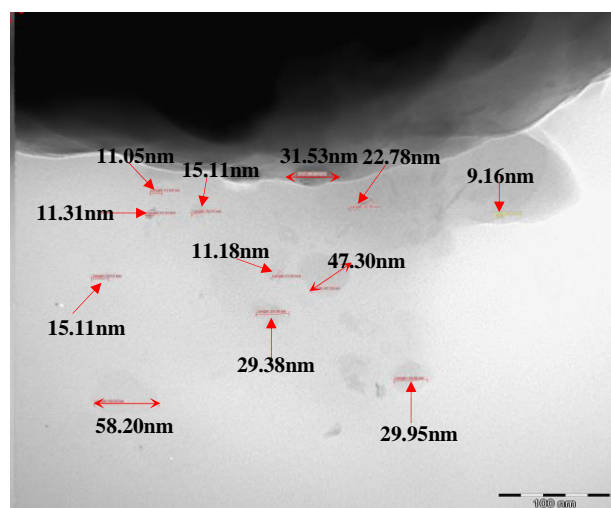


Fig. 5. TEM image of CLNPs milled for 72 hours.

The average particle size that was obtained after 72 hours of milling was 12.88 ± 0.64 nm for CLNPs. The particle size distribution for the TEM image for the CLNPs is represented in Fig. 6. The particle size distribution shows that majority of the particle size were within the range of 20 nm.

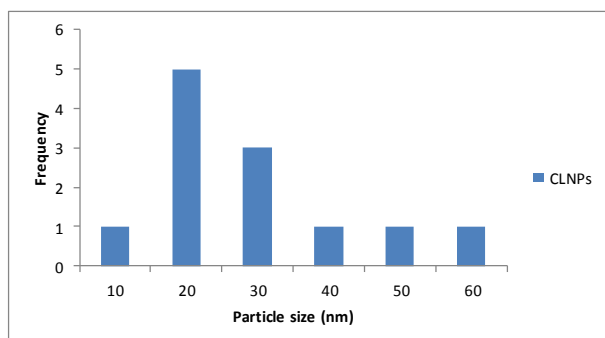


Fig. 6. Particle size distribution obtained from TEM for CLNPs milled for 72 hours.

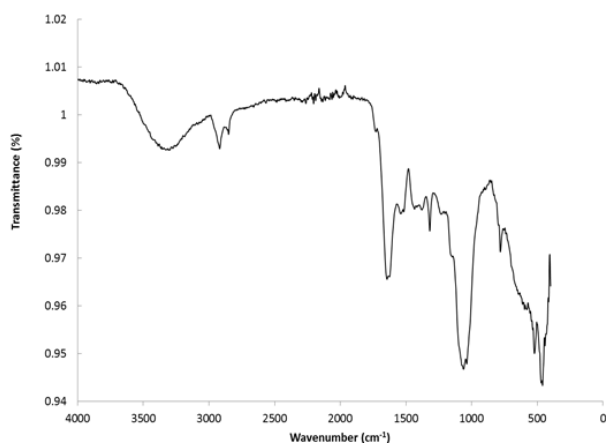


Fig. 7. FTIR Result for CLNPs.

Figure 7 shows the FTIR spectra of cassava leaf. The absorption peak of wave length 2929 and 2856 cm^{-1} , which represent the C-H stretching vibration, are clearly seen, while for the absorption peak at 2268 and 2206 cm^{-1} represents C=N stretching vibration, the absorption peak at 1739 cm^{-1} represents C=O stretching vibration, and the absorption peaks at 1651 cm^{-1} represents C=C bending vibration. The absorption peak at 1548 cm^{-1} represents N-O asymmetric stretching, then the absorption peak at 1444 and 1392 cm^{-1} represents C-C stretching vibration in aromatics and C-H bending vibration and the absorption peaks at 1317 , 1080 and 778 cm^{-1} which indicates C-N stretching vibration, C-O-H stretching in secondary alcohols and weak band N-H out of plane bending, respectively. The absorption peak at 600 , 528 and 464 cm^{-1} represents C=O

out of plane bending, C=C=O bending of carboxylic group and C-N-C bending in amines groups, respectively.

Table 2. List of organic compound from GCMS of CSNPs obtained after milling for 72 hours.

Peak#	R. Time	Area %	Height %	A/H	Name
1	11.669	16.63	11.75	4.80	7-Oxabicyclo [4.1.0] heptane, 1-methyl-4- (2-methyloxiranyl)
2	12.188	3.33	3.75	3.01	4-Methylcatechol, diacetate
3	12.564	15.28	26.24	1.97	1-Octadecyne
4	12.618	1.88	3.45	1.84	Propanoic acid, 2-methyl-, 2-propenyl ester
5	12.853	1.92	3.29	1.98	1-Octyne
6	13.087	3.73	5.86	2.15	1-Nonyne
7	15.316	0.58	1.35	1.46	1H-Tetrazole, 1-phenyl
8	16.198	8.58	12.87	2.26	Phytol
9	19.636	0.89	1.42	2.13	Pentanoic acid, 4-oxo-, pentyl ester
10	19.767	4.89	6.06	2.74	Butanamide
11	26.722	4.96	4.02	4.18	2,4,6-Trimethyl-1-nonene
12	27.024	7.84	7.12	3.73	2-Piperidinone, N-[4-bromo-n-butyl]
13	34.487	29.49	12.81	7.80	A-Norcholestan-3-one, 5-ethenyl-, (5.beta.)
		100	100		

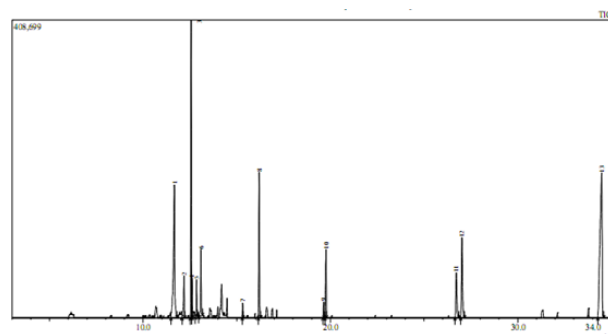


Fig. 8. GC-MS Result of CLNPs.

Table 2 and Fig. 8 shows GCMS result obtained for cassava stem in which the following organic compounds were found: 7-Oxabicyclo [4.1.0] heptane, 1-methyl-4- (2-methyloxiranyl) - has low odour and applications includes metal coatings, varnishes, and printing inks. 4-Methylcatechol, diacetate is an alkaloid, 1-Octadecyne, Propanoic acid, 2-methyl-, 2-propenyl ester, 1-Octyne is a subgroup from the group of alkynes. It consists of several isomeric compounds having the formula C_8H_{14} , 1-Nonyne, 1H-Tetrazole, 1-phenyl-, Phytol, Pentanoic acid, 4-oxo-, pentyl ester. Butanamide is classified as amide and 2, 4, 6-Trimethyl-1-nonene, 2-Piperidinone, N- [4-bromo-n-butyl]-, A-Norcholestan-3-one, 5-ethenyl-, (5.beta.)-. All

these organic compounds fall under the following classes which helps improve the properties of metallic coatings, such as fats, waxes, alkaloids, proteins, phenolics, simple sugars, pectins, mucilages, gums, resins, terpenes, starches, glycosides, saponins, and essential oils [37].

4. CONCLUSION

CLNPs were obtained after ball milling for 60 hours, the average particle size were estimated by SEM/Gwyddion software, XRD and TEM. There was significant decrease in particle size as the milling time increased from 36 to 72 hours. The EDX result revealed trace elements such as O, Si, Ca, K, Fe and S, which are heteroatoms can be added to coatings to help in inhibiting corrosion on metal surfaces. Elements like Si and Ca would improve the strength of coatings as well as reduce corrosion rate of coated metals. XRD result revealed compounds such as SiO_2 , CaCO_3 , $\text{Ca}_2(\text{SO}_4)_2\text{H}_2\text{O}$ and $\text{CaC}_2\text{O}_4(\text{H}_2\text{O})$ these compounds would help in improving the mechanical properties of alloys or composites and coatings. SiO_2 if added to coatings will improve the coating hardness, while the presence of CaCO_3 in coatings will form a precipitate that will serve as a protective film on the surface of the metal, thereby protecting the metal from corrosion. TEM image reveals more precise particle size compared to that obtained from SEM/Gwyddion software and XRD. FTIR result revealed the nature of bond that exist in the CLNPs and GC-MS result showed various organic compounds that were present in the CLNPs. These organic compounds can be classified as fats, waxes, alkaloids, proteins, phenolics, simple sugars, pectins, mucilages, gums, resins, terpenes, starches, glycosides, saponins and essential oils. All of which helps improve the properties of metallic coatings. This work shows that the CLNPs can be produced, and they can be used as additives to coatings for corrosion protection, especially coatings for oil and gas applications. Therefore, CL should not be left to waste as they are useful for additives in coatings. These will add value to the CL that is usually dumped in the environment and also reduces environmental pollution.

Acknowledgement

The authors will like to acknowledge Dr. Abdulhakeem Bello, Physics Department, University of Pretoria, South Africa, Dr. Victor Sunday Aigbodion, Department of Metallurgical and Materials Engineering, University of Nigeria, Nsukka, Nigeria who both assisted in the characterization and Mr. Elakhame in the Ceramic Department in FIRO.

REFERENCES

- [1] S.O. Aro, 'Improvement in the Nutritive Quality of Cassava and Its By-products through Microbial Fermentation - Review', *African Journal of Biotechnology*, vol. 7, no. 25, pp. 4789-4797, 2008.
- [2] A.R. Adetunji, D.A. Isadare, K.J. Akinluwade, O.O. Adewoye, 'Waste-to-Wealth Applications of Cassava-A Review Study of Industrial and Agricultural Applications', *Advances in Research*, vol. 4, no. 4, pp. 212-229, 2015.
- [3] FAOSTAT: 'Production, Crops, Cassava, 2010 data', *Food and Agriculture Organization*, pp. 1 - 11, 2012.
- [4] United Nations Environment Programme, 'Converting Waste Agricultural Biomass into a Resource', *Compendium of Technologies*, pp. 1 - 441, 2009.
- [5] T.I.N. Ezeji, U.E. Eneba, C. Ogueke, 'Waste to Wealth - Value Recovery from Agro-food Processing Wastes Using Biotechnology: A Review', *British Biotechnology Journal*, vol. 4, no. 4, pp. 418-481, 2014.
- [6] O. Akaranta, 'Agro Wastes Utilization: the Chemist's Input', 55th Inaugural Lecture at University of Port Harcourt, pp. 1 - 47, 2007.
- [7] H.A. Abba, I.Z. Nur, S.M. Salit, 'Review of Agro Waste Plastic Composites Production', *Journal of Minerals and Materials Characterization and Engineering*, vol. 1, pp. 271-279, 2013.
- [8] P. Prasertsan, S. Prasertsan, A.H. Kittikun, 'Recycling of Agro-Industrial Wastes through Cleaner Technology', *Biotechnology*, vol. x, pp. 1 - 11, 2010.
- [9] S. Ibrahim, E. Mumtaz, 'Application of Agro-Waste Products as Organic and Value Added Bio-fertilizer for Improving Plant Growth', *Journal of Pharmacy and Clinical Science*, vol. 8, pp. 35 - 41, 2014.
- [10] T.I.N. Ezeji, A.N. Ezeji, A.C. Udebuani, E.U. Ezeji, E.A. Ayalogbu, C.O. Azuwu, L.A.

- Adjero, C.E. Ihejirika, C.O. Ujowundu, L.A. Nwaogu, K.O. Ngwogu, 'Environmental Metals Pollutants Load of a Densely Populated and Heavily Industrialized Commercial City of Aba, Nigeria', *Journal of Toxicology and Environmental Health Science*, vol. 5, no. 1, pp. 1-11, 2013.
- [11] South Pacific Applied Geosciences Commission, 'Agricultural Waste Management and Waste Management Issues for the Pacific and its Impact on their Sustainable Development', pp. 1 - 47, 2010. Accessed on 19 February, 2015.
- [12] United Nations Environment Programme, 'Waste Investing in Energy and Resource Efficiency Toward a Green Economy', pp. 1 - 24, 2011.
- [13] F. Zucchi, I.H. Omar, 'Plant Extracts as Corrosion Inhibitors of Mild Steel in HCl Solutions', *Surface Technology*, vol. 24, no. 4, pp. 391-399, 1985.
- [14] A. Ostovari, S.M. Hoseinieh, M. Peikari, S.R. Shadizadeh, S.J. Hashemi, 'Corrosion Inhibition of Mild Steel in 1 M HCl Solution by Henna Extract: A Comparative Study of the Inhibition by Henna and its Constituents (Lawsonic acid, β -D-Glucose and Tannic acid)', *Corrosion Science*, vol. 51, no. 9, pp. 1935-1949, 2009.
- [15] M. Dahmani, A. Et-Touhami, S.S. Al-Deyab, B. Hammouti, A. Bouyanzer, 'Corrosion Inhibition of C38 Steel in 1 M HCl: A Comparative Study of Black Pepper Extract and Its Isolated Piperine'. *International Journal of Electrochemical Sciences*, vol. 5, pp. 1060 - 1069, 2010.
- [16] A.K., Satapathy, G. Gunasekaran, S.C. Sahoo, K. Amit, P.V. Rodrigues, 'Corrosion inhibition by Justicia gendarussa plant extract in hydrochloric acid solution', *Corrosion Science*, Vol. 51, no. 12, pp. 2848-2856, 2009.
- [17] L.Z. Li, 'Computer-aided Modeling of Nanocrystalline Coating to Reduce the Galvanic Corrosion', *Nanoscience and Nanotechnology*, vol. 2 no. 1, pp. 13-15, 2012.
- [18] A.P.I. Popoola, O.E. Olorunniwo, O.O. Ige, 'Corrosion Resistance Through the Application of Anti-Corrosion Coatings', *Developments in Corrosion Protection*, vol. 13, no. 4, pp. 241 - 270, 2014.
- [19] Y. Qian, Y. Li, S. Jungwirth, N. Seely, Y. Fang, X. Shi, 'The Application of Anti-Corrosion Coating for Preserving the Value of Equipment Asset in Chloride-Laden Environments: A Review', *International Journal of Electrochemical Science*, vol. 10, no. 7, pp. 10756 - 10780, 2015.
- [20] J. Hu, Y. Ji, Y. Shi, F. Hui, H. Duan, M. Lanza, 'A Review on the use of Graphene as a Protective Coating against Corrosion', *Annals of Materials Science & Engineering*, vol. 1, no. 3, pp. 1 - 16, 2014.
- [21] D.M. Lenz, M. Delamar, C.A. Ferreira, 'Improvement of the anticorrosion properties of polypyrrole by zinc phosphate pigment incorporation', *Progress in Organic Coatings*, vol. 58, , no.4, pp. 64-69, 2007.
- [22] U.K. Mudali, S. Ningshen, A.R. Shankar, 'Nanostructured coatings for corrosion protection in reprocessing plants', *Pure Applied Chemistry*, vol. 83, No. 11, pp. 2079-2087, 2011.
- [23] S.A. Bello, J.O. Agunsoye, S.B. Hassan, M.G. Zebase Kana, I.A. Raheem, 'Epoxy Resin Based Composites, Mechanical and Tribological Properties: A Review', *Tribology in Industry*, vol. 37, no. 4, pp. 500 - 524, 2015.
- [24] E. Zdravecká, M. Marton, A. Gmitterko, J. Tkáčová, 'Triboanalysis in Industry for PVD-coated Stamping Dies', *Tribology in Industry*, vol. 36, no. 1, pp. 3 - 8, 2014.
- [25] P.C. Mishra, Prakhardeep, S. Bhattacharya, P. Pandey, 'Finite Element Analysis for Coating Strength of a Piston Compression Ring in Contact with Cylinder Liner: A Tribodynamic Analysis', *Tribology in Industry*, vol. 37, no. 1, pp. 42 - 54, 2015.
- [26] S. Horikoshi, N. Serpone, 'Microwaves in Nanoparticle Synthesis', First Edition, Published 2013 by Wiley-VCH Verlag GmbH & Co. KGaA, pp. 1 - 21, 2013.
- [27] P. Holister, J. Waneer, C.R. Vas, T. Harper, 'Nanoparticles: Technology White Papers', Published by Cientifica, no. 3, pp. 1 - 14, 2003.
- [28] Mandal, 'Synthesis of Nanoparticles', <http://www.news-medical.net/health/Synthesis-of-Nanoparticles.aspx>, 2012. (accessed 14th February, 2015).
- [29] A. Mathiazhagan, R. Joseph, 'Nanotechnology-A New Prospective in Organic Coating - Review', *International Journal of Chemical Engineering and Applications*, vol. 2 no. 4, pp. 225 - 237, 2011.
- [30] S.A. Bello, J.O. Agunsoye, J. A. Adebisi, F.O. Kolawole, S.B. Hassan, 'Physical Properties of Coconut Shell Nanoparticles', *Kathmandu University Journal of Science, Engineering and Technology*, vol. 12 no. 1, pp. 63-79, 2016.
- [31] X. Shi, T.A. Nguyen, Z. Suo, Y. Liu, R. Avci, 'Effect of Nanoparticles on the Anticorrosion and Mechanical Properties of Epoxy Coating', *Surface and Coating Technology*, vol. 204, pp. 237-245, 2009.
- [32] T.P. Chou, C. Chandrasekaran, S. Limmer, C. Nguyen, G.Z. Cao, 'Organic-Inorganic Sol-gel Coating for Corrosion Protection of Stainless Steel', *Journal of Materials Science Letter*, vol. 21, pp. 251-255, 2002.

- [33] H. Shi, F. Liu, E. Han, Y. Wei, 'Effects of Nano Pigments on the Corrosion Resistance of Alkyd Coating', *Journal of Materials Science and Technology*, vol. 23, no. 4, pp. 551-558, 2007.
- [34] R.K. Rajput, 'Material Science and Engineering', S. K. Kataria & Sons, Nai – Saraki, Delhi, pp. 854 – 872, 2006.
- [35] M.D. Holloway, C. Nwaoha, O.A. Onyewuenyi, 'Process Plant Equipment: Operation, Control, and Reliability', First Edition. Published 2012 by John Wiley & Sons, Inc, pp. 1 – 76, 2012.
- [36] A. Monshi, M.R. Foroughi, M.R. Monshi, 'Modified Scherrer Equation to Estimate More Accurately Nano-Crystallite Size Using XRD', *World Journal of Nano Science and Engineering*, vol. 2, pp. 154-160, 2012.
- [37] D. Mohan, C.U. Pittman, P.H. Steele, 'Pyrolysis of Wood/Biomass for Bio-Oil: A Critical Review', *Energy & Fuels*, vol. 20 no. 3, pp. 848-889, 2006.